Modeling crack nucleation at coherent twin boundaries in nickel-based superalloys

Conference Paper · October 2013

CITATIONS
4

READS
123

6 authors, including:

Ashley Spear
University of Utah
10 PUBLICATIONS **38** CITATIONS
SEE PROFILE

Joseph C Tucker
Exponent
9 PUBLICATIONS **59** CITATIONS
SEE PROFILE

A.D. Rollett
Carnegie Mellon University
391 PUBLICATIONS **6,241** CITATIONS
SEE PROFILE

A.R. Ingraffea
Cornell University
243 PUBLICATIONS **5,315** CITATIONS
SEE PROFILE

MODELING CRACK NUCLEATION AT COHERENT TWIN BOUNDARIES IN NICKEL-BASED SUPERALLOYS

Albert Cerrone[1], Ashley Spear[1], Joseph Tucker[2],
Clayton Stein[2], Anthony Rollett[2], Anthony Ingraffea[1]

[1] School of Civil and Environmental Engineering, Cornell University, Ithaca, NY
[2] Department of Materials Science and Engineering, Carnegie Mellon University, Pittsburgh, PA

Keywords: LSHR, Twin, Nucleation

Abstract

Nickel-based superalloys are used widely in gas turbine engines for their excellent tensile strength and creep resistance at high temperatures. To improve damage assessment measures and aid in the design of next generation materials, there is a necessity to understand the fatigue cracking processes down to the microstructural scale. Microcrack nucleation in superalloys such as LSHR is presumed to be caused by slip localization due to the buildup of incompatibility stresses close to long coherent twin boundaries. To account numerically for this mechanism, a crystal plasticity model was applied wherein twin-parallel slip systems were favored for slip more so than non-twin-parallel systems both implicitly and explicitly. Upon verifying its ability to accommodate relatively high amounts of slip on twin-parallel systems, the crystal plasticity model was applied to a three-dimensional finite element model of the reconstruction of LSHR from high energy X-ray diffraction microscopy (HEDM). Preliminary numerical observations and details of the crystal plasticity model, the characterization of LSHR using HEDM, and the model-making procedure are included herein.

Introduction

Annealing twins are often referred to as strengtheners in the microstructure as their high-angle, low-energy boundaries tend to prevent the transmission of dislocations [1]. Heavily twinned microstructures do not necessarily exhibit the classic Hall-Petch strengthening relation, and work has been done to quantify the twins' influence on the grain-size effect. Konopka and Wyrzykowski [2] developed a relation for yield stress based on the frequency of twin boundaries that strongly or weakly oppose dislocation movement and those that act as dislocation sources. Pande *et al.* [3] modified the Hall-Petch relation by assuming all twin boundaries act as barriers to dislocation motion (in slight opposition to Li's [4] grain boundary strengthening arguments in which boundaries are assumed to emit dislocations) and incorporating an effective grain size term accounting for the presence of twin boundaries. Regardless of whether dislocations are prevented from transmitting across twin boundaries or are emitted from them, there is no question that dislocation pileup at twin boundaries poses severe consequences for the material's ability to resist microcrack nucleation.

It has been established that microcracks tend to nucleate at the twin boundaries of certain FCC materials such as nickel alloys [5, 6] and copper [7, 8]. Why are twin boundaries favorable sites for fatigue crack formation? Heinz and Neumann [9] argued that elastic anisotropy and coherency are decisive. First, high stress concentrations develop at the twin boundaries due to elastic anisotropy. These high stresses, in turn, which can be estimated using the closed-form

solution of Neumann [10], facilitate glide at the boundaries. It is noteworthy that these high incompatibility stresses do not produce additional shear stress on the boundary plane. Rather, a logarithmic stress singularity develops where the free surface and twin boundary trace meet. Second, alignment of the twin boundary and a slip plane (as with a coherent twin boundary) allows for dislocations to travel relatively far distances unhindered, rendering high strains under such high incompatibility stresses. Several studies have been conducted which support these claims. Miao *et al.* [5], for example, observing the nickel-based superalloy René88DT [11] under high cycle fatigue loading, found that microcracks tended to initiate close to coherent twin boundaries in large, high-Schmid factor (soft) grains. Stein *et al.* [6], investigating the nickel-based superalloy LSHR [12], also found that microcracks nucleated at coherent Σ3 boundaries with larger than average chord lengths at the surface.

To account numerically for these physical mechanisms, a methodology is proposed wherein high fidelity finite element models are generated from 3D high-energy X-ray diffraction microscopy (HEDM) reconstructions and coupled with a grain-size sensitive crystal plasticity model. The first part of this paper will detail the formulation of the crystal plasticity model and explore its viability in accommodating relatively high amounts of slip on twin-parallel systems. The second part will detail the LSHR characterization effort, the steps necessary to produce a three-dimensional finite element model from a 3D HEDM dataset, and preliminary simulation efforts.

Crystal Plasticity Modeling Considerations

Crystal Plasticity Model Formulation

The elasto-viscoplastic crystal plasticity model follows the formulation given by Matouš and Maniatty [13]. It is implemented for FCC with twelve octahedral, {1 1 1}, and six cubic, {1 1 0}, slip systems. The resolved shear stress τ on slip system α is given by:

$$\tau^{\alpha} = \mathbf{s}^{\alpha}[\mathbf{C}^{e}\mathbf{S}]\mathbf{m}^{\alpha} \quad , \tag{1}$$

where **m** is the slip plane normal, **s** the slip direction, $\mathbf{C}^{e}$ the Cauchy Green Tensor, and **S** the 2nd Piola-Kirchoff Stress. The slip rate along the slip systems is given by

$$\dot{\gamma^{\alpha}} = \dot{\gamma_o} \frac{\tau^{\alpha}}{g^{\alpha}} \left| \frac{\tau^{\alpha}}{g^{\alpha}} \right|^{\frac{1}{m}-1} \quad , \tag{2}$$

where $\dot{\gamma^{\alpha}}$ and $\dot{\gamma_o}$ are the shear and reference shear rates, respectively, m is a material rate sensitivity parameter, and g the hardness. Hardness evolves according to a grain-size sensitivity term given by Beaudoin *et al*. [14] and a Voce-Kocks [15, 16] relation, the first and second terms in Equation 3, respectively.

$$\dot{g^{\alpha}} = H_o \frac{\beta^2 \mu^2 b}{2(g^{\alpha} - g_o^{\alpha})} \sum_{\kappa=1}^{N_{ss}} \sqrt{\Delta_{ij} m_j \Delta_{kL} m_L} |\dot{\gamma^{\kappa}}| + G_o \left(\frac{g_s^{\alpha} - g^{\alpha}}{g_s^{\alpha} - g_o^{\alpha}} \right) \sum_{\kappa=1}^{N_{ss}} |\dot{\gamma^{\kappa}}| \quad , \tag{3}$$

H_o and G_o in Equation 3 are rate coefficients, $\beta = 1/3$, b is the Burgers vector, and g_o and g_s are initial and saturation resolved shear strengths, respectively. The Δ variable in the first term of

the hardness evolution is a dislocation density term, a measure of lattice incompatibility, and is expressed as a function of the plastic deformation:

$$\Delta_{iJ} = \boldsymbol{\epsilon}_{JKL}\mathbf{F}^{p}_{iL,K} \tag{4}$$

This measure is appropriate for modeling annealing twins because high gradients of plastic deformation develop across their boundaries. Consequently, geometrically-necessary dislocations localize close to the boundaries to accommodate these high gradients [17]. The Δ term effectively accounts for this phenomenon by considering the gradient of the plastic deformation gradient, accommodating the evolution of slip close to twin boundaries. It is noteworthy that the Voce-Kocks relation in Equation 3 is a slight departure from that given in the original formulation of the crystal plasticity model [13]. Here, latent and self-hardening effects are not assumed equal; consequently, the slip systems do not harden at the same rate. This is to allow the preference for slip on the twin-parallel systems discussed earlier.

Optionally, to supplement the implicit hardening effects of the model, the critical resolved shear stress values assigned to twin-parallel systems are scaled to be lower than those of non-twin-parallel systems. The idea here is that for systems with relatively long slip line lengths (as with twin-parallel systems), the lower critical resolved shear stress facilitates the evolution of slip on those systems, thereby replicating physically observed phenomena. To accomplish this, the four {111} slip planes are centered at the grain's centroid. For each slip plane, the shortest distance between the centroid and trace of grain surface on the slip plane is recorded. The scaling, finally, is accomplished by considering the ratio of the longest slip line length to the shortest. Twin lamellae exhibit the highest ratios (~6) while equi-axed grains show no preference, meaning that this scaling only effects grains with elongated morphologies.

The Baseline Model

A relatively simple, idealized finite element model of a twin lamella and its containing grain was generated for the purposes of probing the sensitivity of slip localization to orientation, twin lamella length, and twin-containing grain size, offering a means to gauge the effectiveness of the crystal plasticity model at accommodating slip on twin-parallel systems. The twin and its containing grain, surrounded by a cubical as-large-as (ALA) grain for load-transfer purposes, could be assigned orientations to yield coherent twin boundaries, Figure 1.

A baseline model with coherent twin boundaries is considered here. Figure 2(a) shows accumulated slip on the twin lamella without the scaling discussed earlier. It is apparent that slip evolved from the lamella's edges inward. Moreover, approximately 80% of total slip on the twelve octahedral slip systems was on the twin-parallel systems. A baseline model without the twin lamella is considered next to gauge the crystal plasticity model's ability to accommodate slip on twin-parallel systems without long, slender twin morphologies. Here, the twin lamella, labeled B in Figure 1, was merged into half of the twin-containing grain, region C, leaving a coherent $\Sigma 3$ boundary between grains BC and A. Figure 2(b) and Figure 2(c) show the evolution of slip in grain A without and with scaling of the twin parallel systems, respectively. Without scaling, approximately 75% of total slip on the octahedral slip systems was on the boundary-parallel systems. With scaling, this percentage rose to 80%. For all three of these simulations, it is noteworthy that the highest localizations of slip occurred at the coherent boundaries. One

could extend this observation to the idea of hotspots and the identification of potential microcrack nucleation sites [18].

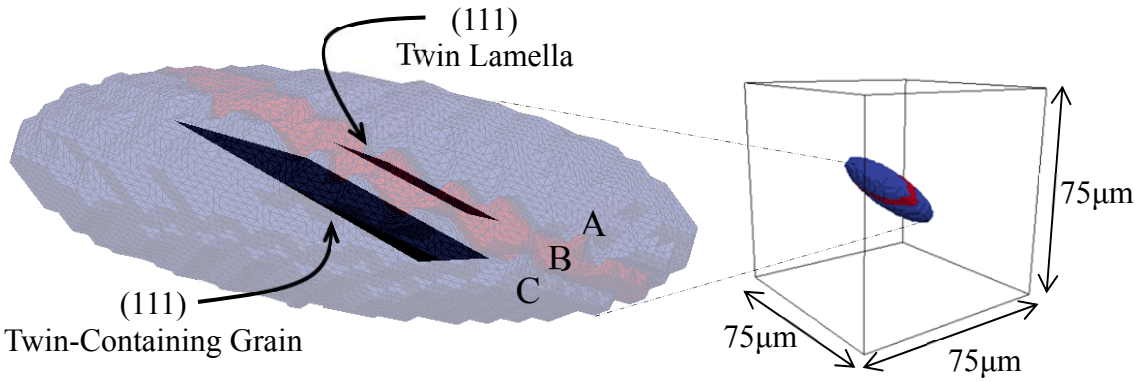

Figure 1. The baseline model showing alignment of the (111) slip planes of the twin lamella and twin-containing grain with the twin boundaries, rendering coherent twin boundaries.

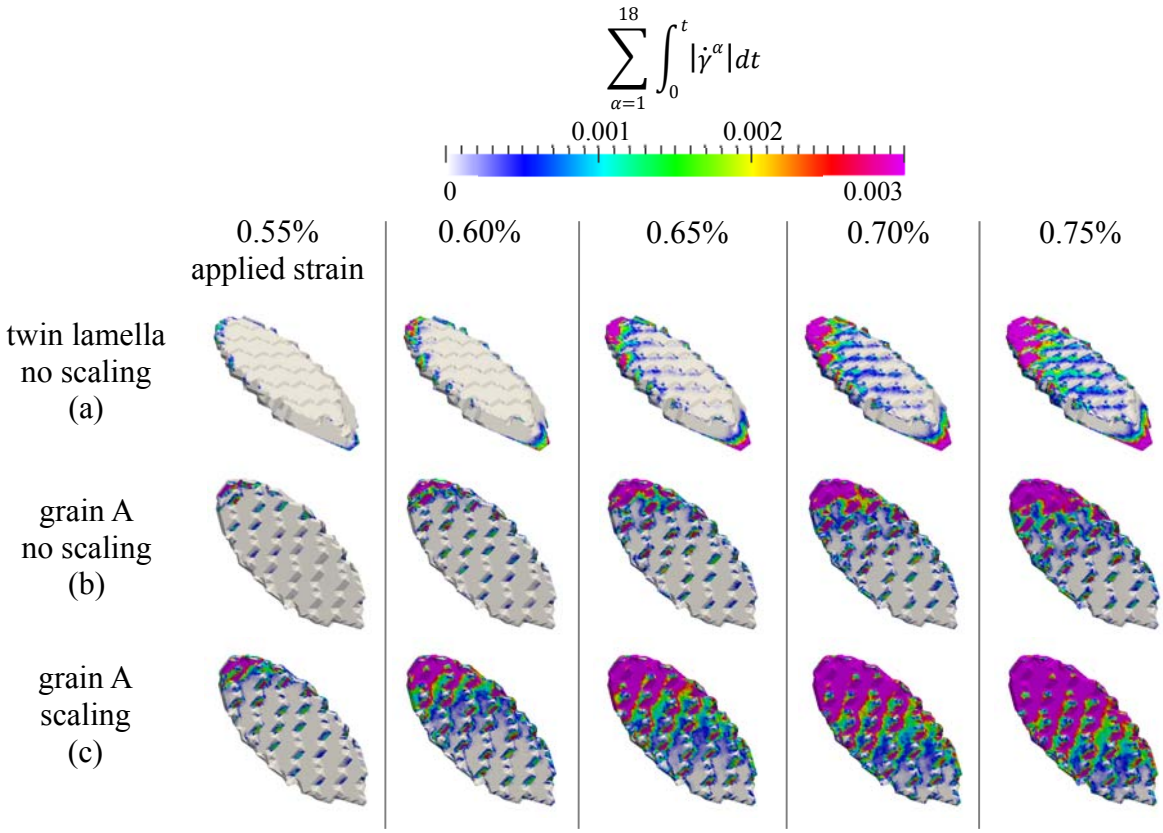

Figure 2. Evolution of slip in baseline model on twin lamella without scaling (a), grain A without twin lamella and no scaling (b), and grain A without twin lamella and with scaling (c).

LSHR Reconstruction

Characterization

The alloy LSHR, low-solvus high-refractory, is noted for its exceptional tensile strength and creep resistance at high temperatures, making it a desirable material for use in aircraft gas turbine engines. This powder metallurgy material happens to have a considerable degree of annealing twins in the microstructure, making it an appropriate material for this study. A sample of LSHR subjected to 37,500 cycles of low cycle fatigue loading at room temperature was taken to the Advanced Photon Source at Argonne National Laboratory for characterization with HEDM. The hallmark of this method is that it allows the scientist to obtain both a 3D orientation and spatial mapping nondestructively. The following is a brief description of the collection and reconstruction process, but the reader is directed to Poulsen *et al*. [19] and Suter *et al*. [20] for a more thorough discussion. First, the LSHR sample was loaded on a stage situated between a high-energy X-ray beam source and a CCD camera lens used to capture diffraction from individual grains. The X-ray beam was directed at the sample as the stage rotated about the axis perpendicular to the incident beam. For each rotation, diffraction images were collected. The cross-sectional geometry was then later ascertained from the measured Bragg spots of each rotation. To determine the crystallographic orientations of the grains, a forward modeling reconstruction procedure was employed wherein the data collection procedure was simulated iteratively until a suitable fit was found between experimental and simulated scattering.

A small subsection of the reconstruction alongside an EBSD scan of the same area is shown in Figure 3. A microcrack was identified in the SEM, situated close to a coherent Σ3 boundary. This, to the authors' knowledge, represents the first time a naturally occurring microcrack has been located within a 3D non-destructive orientation map. The two grains along the coherent Σ3 boundary in question are relatively larger and softer than their nearest-neighbors. This observation, to some extent, supports the observations of Miao *et al*. [5] in which microcracks initiate close to twin boundaries in large, high-Schmid factor grains oriented favorably for slip along boundary parallel slip directions.

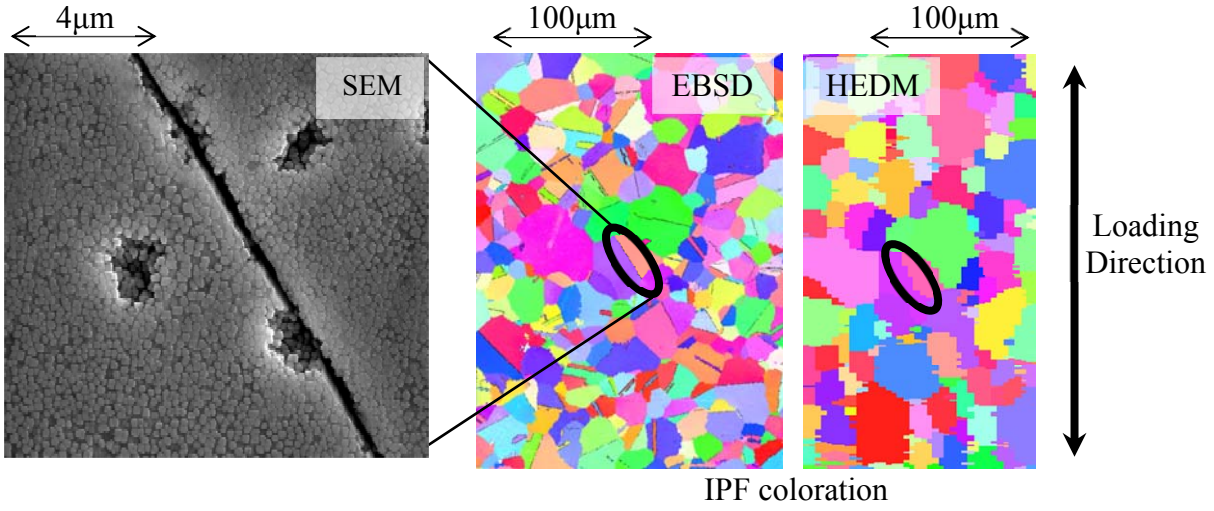

Figure 3. EBSD scan of free surface of LSHR sample alongside its HEDM reconstruction. A portion of the microcrack close to a coherent Σ3 boundary identified in the SEM is shown on the left.

Microstructure Generation And Meshing

The reconstructed volume was imported into the microstructure analysis and generation software DREAM.3D [21] as a .ph file. The resolution was specified to yield an 82.0 x 235.5 x 256.0 μm volume, Figure 4. A multiple-material marching cubes (M3C) [22] algorithm was specified in DREAM.3D to mesh each generated grain. This procedure was preferred over the traditional marching-cubes algorithm as it rendered a surface mesh of the entire volume with conformal grain boundaries without voids or penetrations. The surface mesh of each grain was output in binary stereolithography (STL) files.

A volumetric meshing algorithm given by Cavalcante *et al*. [23, 24] was then exposed for the purposes of discretizing the volume of each grain with tetrahedra. The resulting 1,229-grain mesh was composed of 10,700,578 quadratic tetrahedra. This 45-million degree-of-freedom (DOF) model necessitated the exploitation of a massively parallel finite element driver for use in a high performance computing environment. One such driver used in this investigation was Finite Element All-Wheel Drive (FEAWD), a MPI-based code built on FemLib (a library of constitutive models and finite elements), Boost, the BLAS and LAPACK, PETSc, ParMETIS, and HDF5. Stampede, Texas Advanced Computing Center's Dell Linux cluster, was the primary computational resource used for the simulations discussed in this paper.

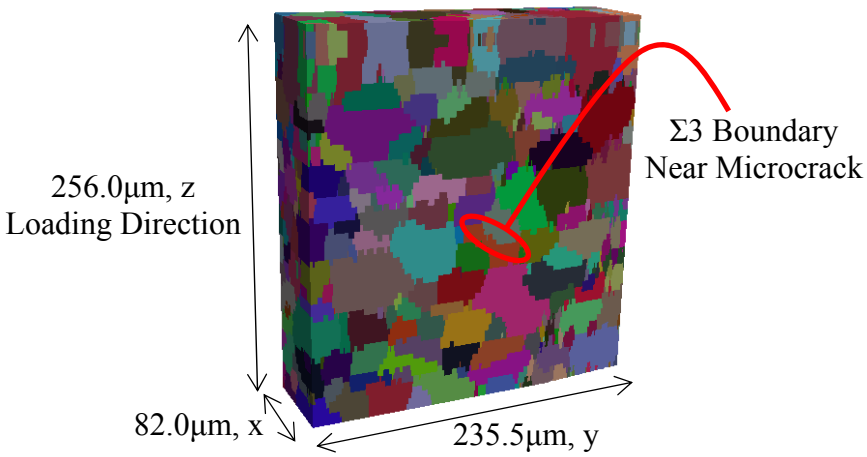

Figure 4. Reconstructed 1,229-grain volume containing the microcrack close to the Σ3 boundary shown in Figure 3.

Simulation

The model was loaded monotonically in simple tension. The grains were assigned orientations from the aforementioned forward modeling reconstruction procedure. Slip began to localize on the free surface at approximately 0.45% applied strain; however, these localizations were not near the coherent Σ3 boundary in question. For increasing load, slip eventually did accumulate near this boundary, but this was after more significant localizations developed elsewhere on the free surface, Figure 5.

Conclusions

From the baseline model simulations, it is evident that accounting for the gradient of the plastic deformation gradient close to twin and coherent Σ3 boundaries in the hardness evolution of the

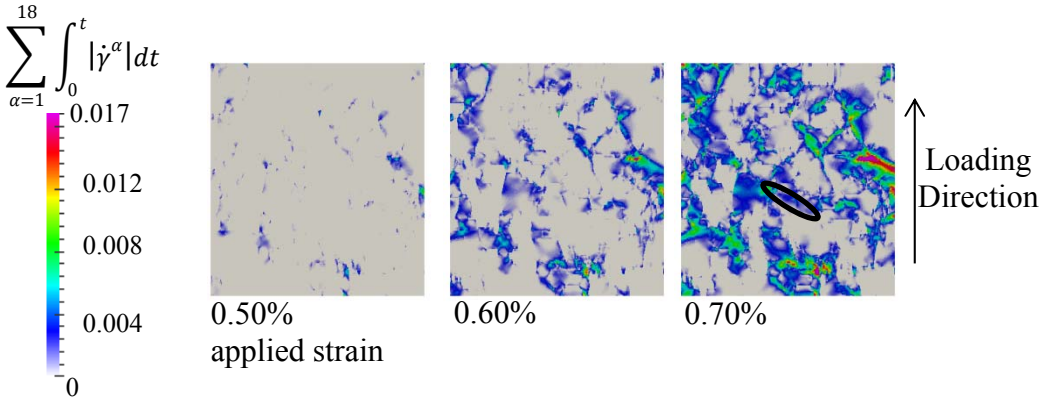

Figure 5. Evolution of slip in reconstruction model. The Σ3 boundary shown in Figure 3 is circled in black.

crystal plasticity formulation is an effective means to accommodate slip on twin-parallel systems. This replicates physically realistic behavior in which incompatibility stresses at these boundaries facilitate the accumulation of slip on preferentially aligned systems, leading to microcrack nucleation. A naturally occurring microcrack along a coherent Σ3 boundary in LSHR, a seemingly favorable site for microcrack initiation, was identified using HEDM. The corresponding three-dimensional reconstruction was meshed for analysis, and the simulation showed no significant localization of slip near the Σ3 boundary in question. Work with this reconstruction is still ongoing.

Acknowledgements

This research was funded by the Air Force Office of Scientific Research under grant number FA9550-10-1-0213, supervised by Dr. David Stargel. Simulations were made possible in part by the National Science Foundation through XSEDE resources.

References

1. L. C. Lim, "Slip-twin interactions in nickel at 573K at large strains," *Scripta Metallurgica*, 18 (10) (1984), 1139–1142.
2. K. Konopka and J. W. Wyrzykowski, "The effect of the twin boundaries on the yield stress of a material," *Journal of Materials Processing Technology*, 64 (1-3) (1997), 223–230.
3. C. S. Pande, B. B. Rath, and M. A. Imam, "Effect of annealing twins on Hall–Petch relation in polycrystalline materials," *Materials Science and Engineering: A*, 367 (1-2) (2004), 171–175.
4. J. C. M. Li, "Petch relation and grain boundary sources," *Trans. TMS-AIME*, 277 (1963), 239–247.
5. J. Miao, T. M. Pollock, and J. Wayne Jones, "Crystallographic fatigue crack initiation in nickel-based superalloy René 88DT at elevated temperature," *Acta Materialia*, 57 (20) (2009), 5964–5974.
6. C. Stein, S. Lee, and A. Rollett, "An Analysis of Fatigue Crack Initiation Using 2D Orientation Mapping and Full-Field Simulation of Elastic Stress Response," in *Superalloys 2012*, Champion, PA, 2012.

7. N. Thompson, N. Wadsworth, and N. Louat, "The origin of fatigue fracture in copper," *Philosophical Magazine*, 1 (2) (1956), 113–126.
8. R. C. Boettner, A. J. McEvily, and Y. C. Liu, "On the formation of fatigue cracks at twin boundaries," *Philosophical Magazine*, 10 (103) (1964), 95–106.
9. A. Heinz and P. Neumann, "Crack initiation during high cycle fatigue of an austenitic steel," *Acta Metallurgica et Materialia*, 38 (10) (1990), 1933–1940.
10. P. Neumann, "Analytical Solution for the Incompatibility Stresses at Twin Boundaries in Cubic Crystals," in in *Fatigue 99*, Beijing, 1999, pp. 107–114.
11. D. Kreuger and R. Kissinger, "Fatigue crack growth resistant nickel-base article and alloy and method for making," US Patent #4957567.
12. T. Gabb, J. Gayda, J. Telesman, and P. Kantzos, "Thermal and mechanical property characterization of the advanced disk alloy LSHR," (2005).
13. K. Matouš and A. M. Maniatty, "Finite element formulation for modelling large deformations in elasto-viscoplastic polycrystals," *International Journal for Numerical Methods in Engineering*, 60 (14) (2004), 2313–2333.
14. A. J. Beaudoin, A. Acharya, S. R. Chen, D. A. Korzekwa, and M. G. Stout, "Consideration of grain-size effect and kinetics in the plastic deformation of metal polycrystals," *Acta Materialia*, 48 (13) (2000), 3409–3423.
15. E. Voce, "A practical strain-hardening function," *Metallurgica*, 51 (307) (1955), 219–226.
16. U. F. Kocks, "Laws for work-hardening and low-temperature creep," *ASME, Transactions, Series H-Journal of Engineering Materials and Technology*, 98 (1976), 76–85.
17. M. F. Ashby, "The deformation of plastically non-homogeneous materials," *Philosophical Magazine*, 21 (170) (1970), 399–424.
18. A. D. Rollett, R. A. Lebensohn, M. Groeber, Y. Choi, J. Li, and G. S. Rohrer, "Stress hot spots in viscoplastic deformation of polycrystals," *Modelling and Simulation in Materials Science and Engineering*, 18 (7) (2010), 074005.
19. H. F. Poulsen, S. F. Nielsen, E. M. Lauridsen, S. Schmidt, R. M. Suter, U. Lienert, L. Margulies, T. Lorentzen, and D. Juul Jensen, "Three-dimensional maps of grain boundaries and the stress state of individual grains in polycrystals and powders," *Journal of Applied Crystallography*, 34 (6) (2001), 751–756.
20. R. M. Suter, D. Hennessy, C. Xiao, and U. Lienert, "Forward modeling method for microstructure reconstruction using x-ray diffraction microscopy: Single-crystal verification," *Review of Scientific Instruments*, 77 (12) (2006), 123905.
21. M. Jackson and M. Groeber, "DREAM.3D," <http://dream3d.bluequartz.net/>.
22. Z. Wu and J. M. Sullivan, "Multiple material marching cubes algorithm," *International Journal for Numerical Methods in Engineering*, 58 (2) (2003), 189–207.
23. J. B. Cavalcante-Neto, P. A. Wawrzynek, T. M. Carvalho, L. F. Martha, and A. R. Ingraffea, "An algorithm for three-dimensional mesh generation for arbitrary regions with cracks," *Engineering with Computers*, 17 (2001), 75–91.
24. J. B. Cavalcante-Neto, L. F. Martha, P. A. Wawrzynek, and A. R. Ingraffea, "A back-tracking procedure for optimization of simplex meshes," *Communications in Numerical Methods in Engineering*, 21 (12) (2005), 711–722.